

Supporting information

1 Characterization of MOF-808

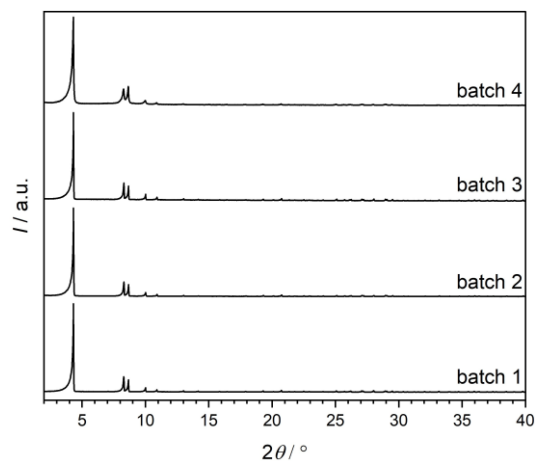


Figure S1: Comparison of the PXRDs for four synthesis batches of MOF-808.

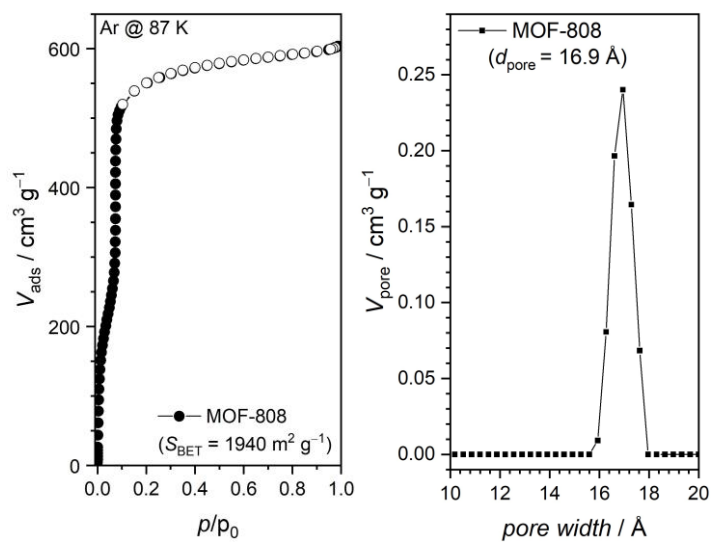


Figure S2: Adsorption isotherm of Ar on MOF-808 at 87 K (left) and the related pore size distribution histogram, with a peak pore diameter of 16.9 Å (right).

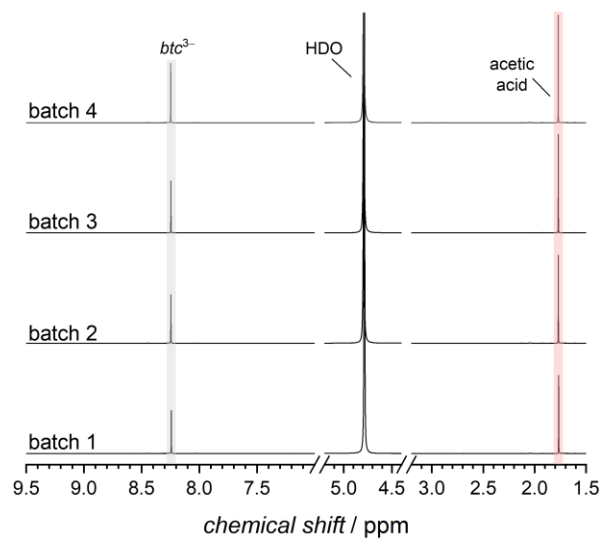


Figure S3: $^1\text{H-NMR}$ spectra for four synthesis batches of MOF-808. Peaks correspond to the chemical shifts of protons in trimesic acid (grey) and acetic acid (red).

2 Characterization of TM-MOF-808

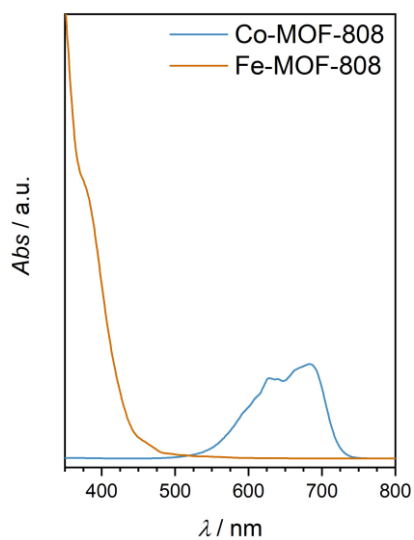


Figure S4: UV-vis spectra of Co- and Fe-MOF-808.

3 Characterization of Eu-MOF-808

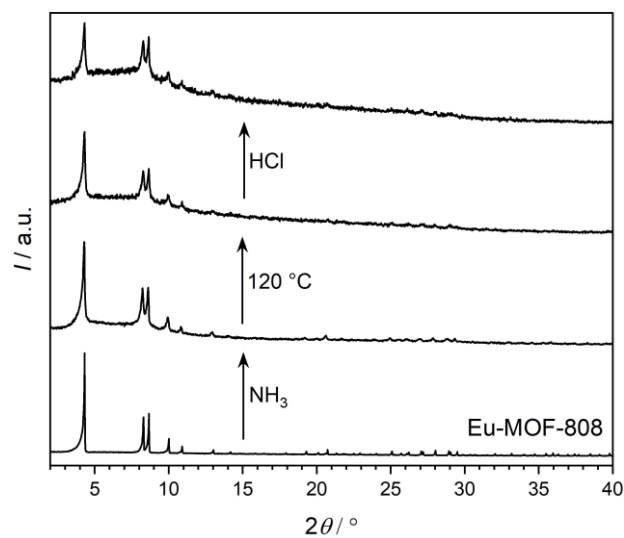


Figure S5: PXRDs of as-synthesized Eu-MOF-808 (bottom), following exposure to NH_3 (second from bottom), after activation at $120\text{ }^\circ\text{C}$ (second from top) and subsequent exposure to gaseous HCl (top).

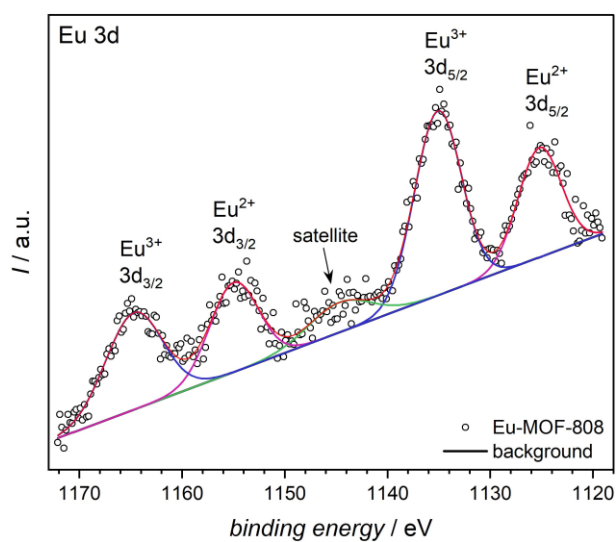


Figure S6: XPS spectrum of as-synthesized Eu-MOF-808 showing peaks correlating to europium ions in the oxidation state +II and +III.

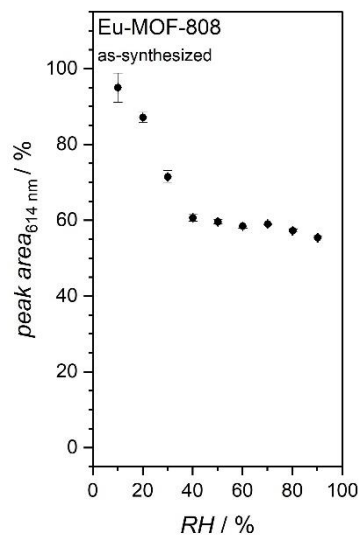


Figure S7: Dependence of the normalized fluorescence peak area (%) on relative humidity (RH) for as-synthesized Eu-MOF-808 referred to the fluorescence intensity at 10% relative humidity.

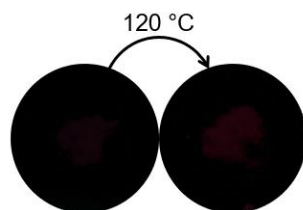


Figure S8: Photographs of as-synthesized Eu-MOF-808 before (left) and after (right) thermal activation at 120 °C, illustrating the absence of visible fluorescence.

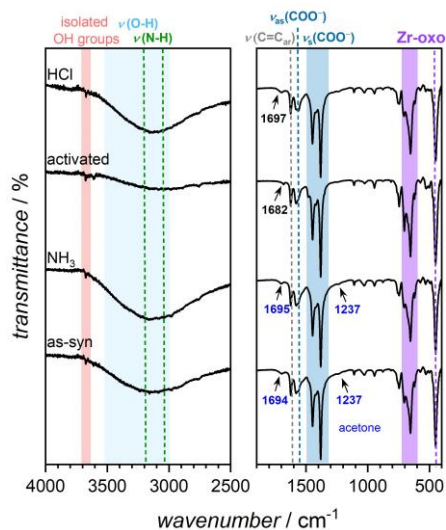


Figure S9: IR spectra of MOF-808 before (as-syn) and after the sequence steps of ammonia exposure, activation at 120 °C and HCl treatment.

4 Characterization of Eu,TM-MOF-808

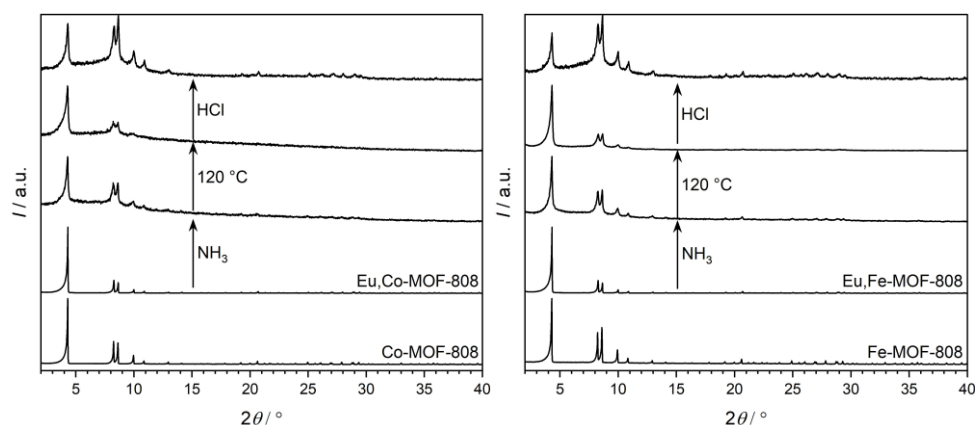


Figure S10: PXRDs of as-synthesized Co- (left) and Fe-MOF-808 (right) before and after the insertion of europium cations. The PXRDs after every step of the defined read-out sequence are also shown.

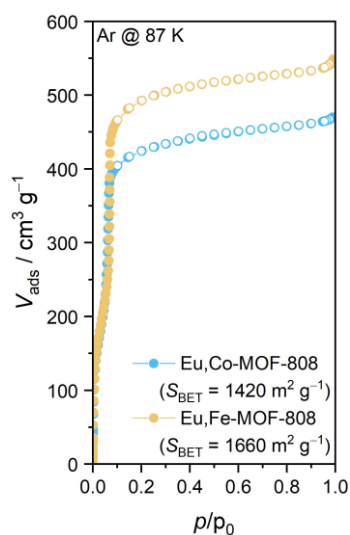


Figure S11: Adsorption isotherms of Ar on Eu,Co- and Eu,Fe-MOF-808 at 87 K.

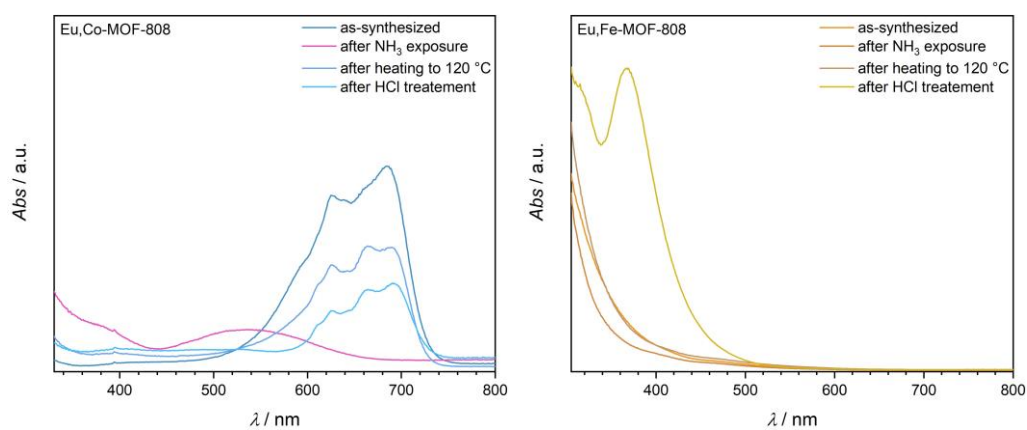


Figure S12: UV-vis spectra of as-synthesized Eu,Co- (left) and Eu,Fe-MOF-808 (right) before and after every step of the read-out sequence.

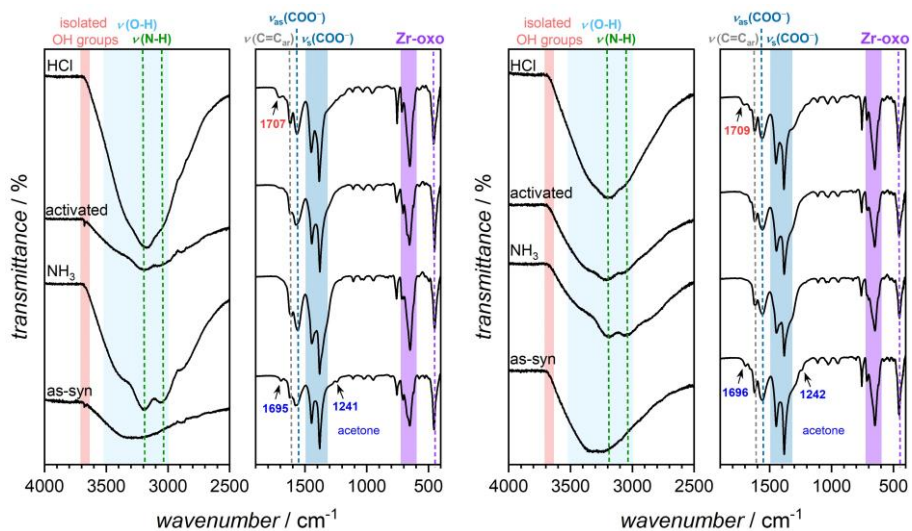


Figure S13: FTIR spectra of Eu,Co- (left) and Eu,Fe-MOF-808 (right) before and after applying the steps of the read-out sequence.

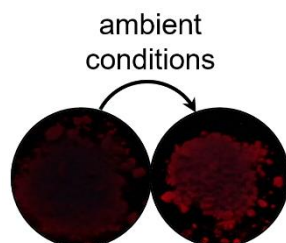


Figure S14: Photographs of Eu,Co-MOF-808 exposed to ammonia and thermally activated before (left) and after (right) storage under ambient conditions, demonstrating increased fluorescence.

5 Characterization of Eu, TM-MOF-808@PVDF

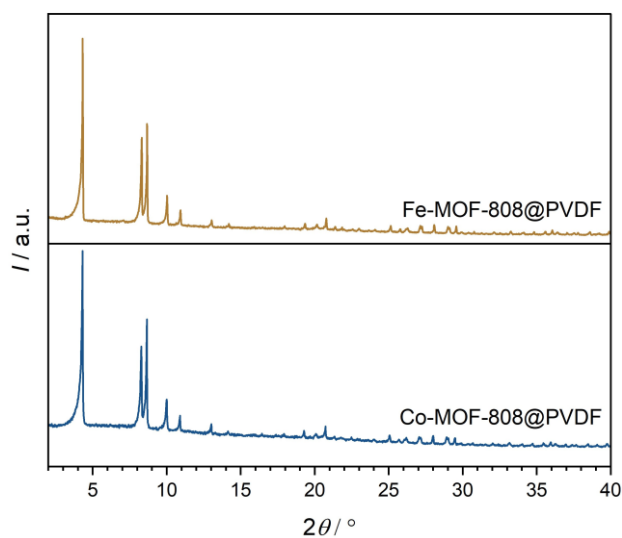


Figure S15: PXRDs of TM-MOF-808@PVDF.

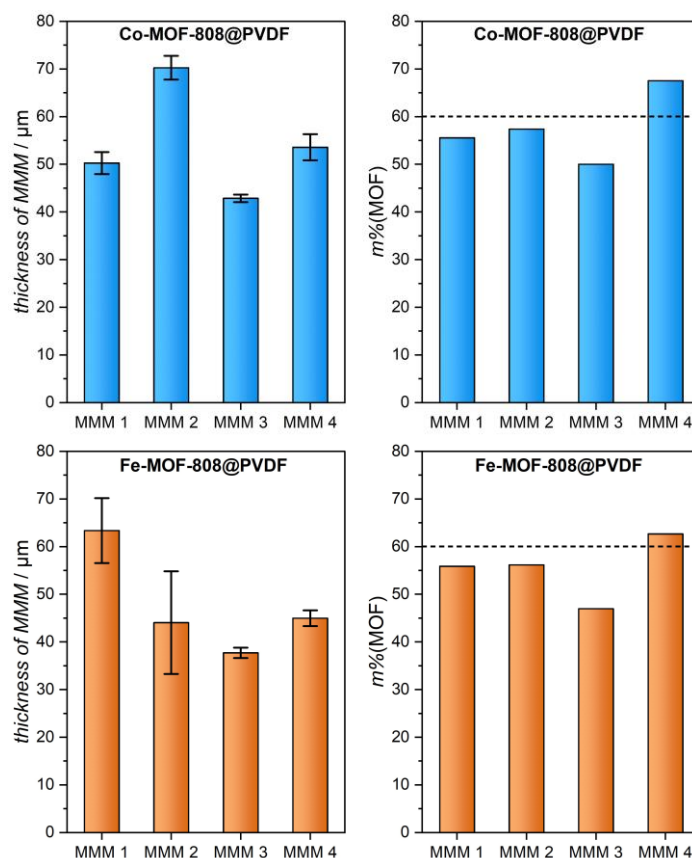


Figure S16: Thickness of four different MMMs of Co- (top left) and Fe-MOF-808@PVDF (bottom left) and the percentage filling of MOF particles within the MMMs, with the dotted lines representing the amount of MOF particles added during preparation (right).

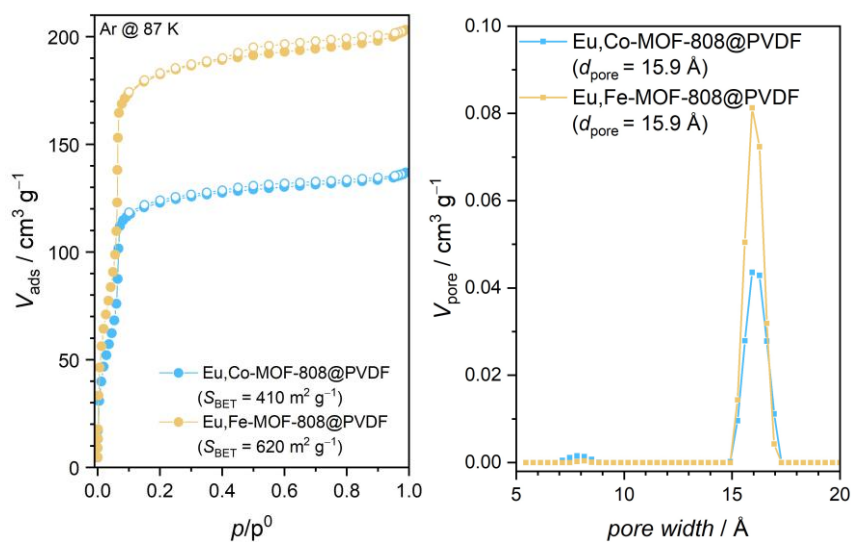


Figure S17: Adsorption isotherm of Ar on Eu, TM-MOF-808 @PVDF at 87 K (left) and the related pore size distribution histogram, with a peak pore diameter of 15.9 \AA (right).

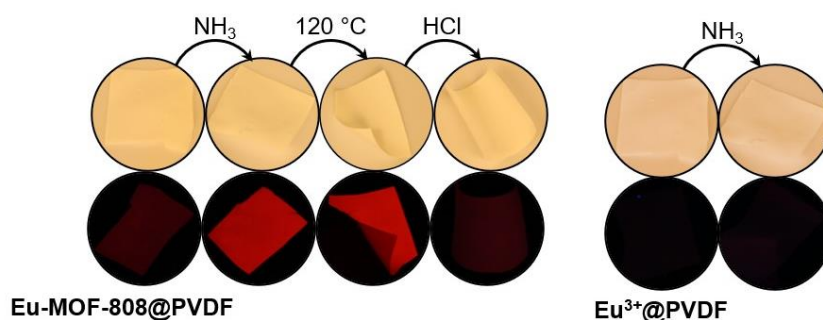


Figure S18: Eu-MOF-808@PVDF fluorescence switching (excitation at 254 nm under UV lamp) by the defined read-out sequence (left) compared to the lack of fluorescence turn-on of the Eu^{3+} -PVDF sample after exposure to NH_3 (right).

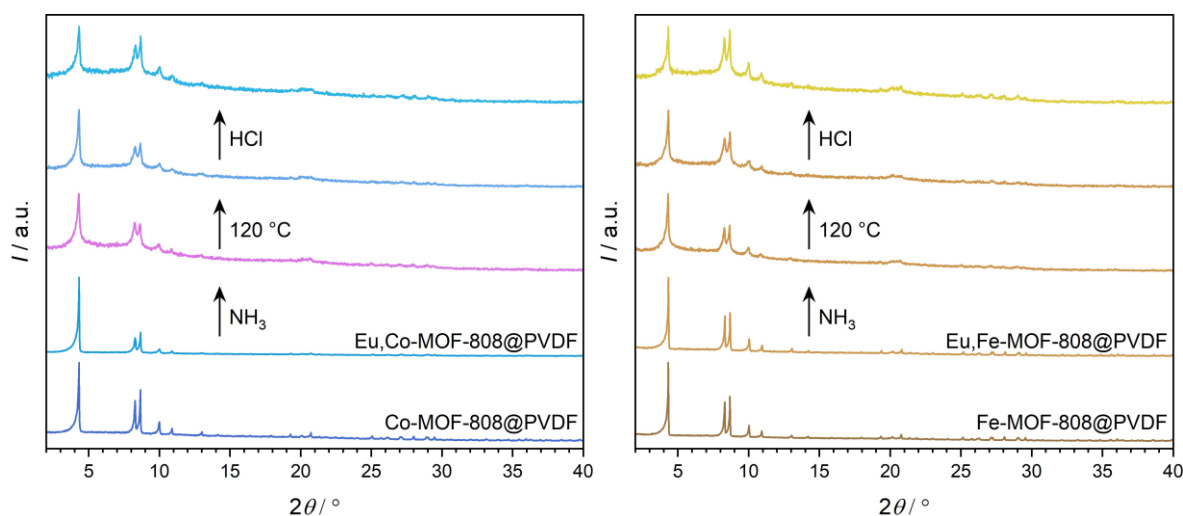


Figure S19: PXRDs of Co- (left) and Fe-MOF-808@PVDF (right) compared to the europium modified samples after every step of the read-out sequence.

5.1 Fluorescence measurements with a portable fluorescence spectrometer

The fluorescence read-out of the MMMs was performed with a portable fluorescence spectrometer which was placed on top of a self-designed measuring cell that was 3D printed (see SI Figure S24). The cell has two gas ports to allow for measurements in an inert environment using nitrogen. To obtain consistent measurements, the MMM was covered with a 3D printed plate featuring a circular groove so that always the same area was excited during the measurement.

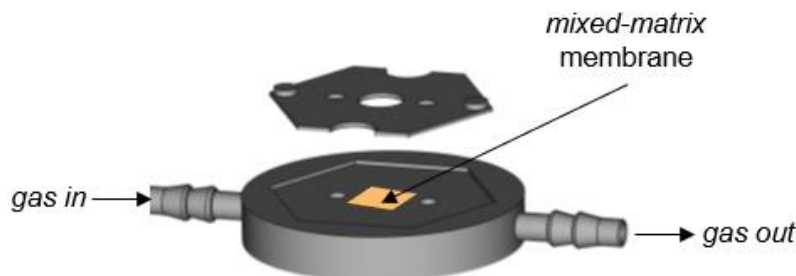


Figure S20: Illustration of a self-designed 3D printed measuring cell used for the fluorescence read-out.

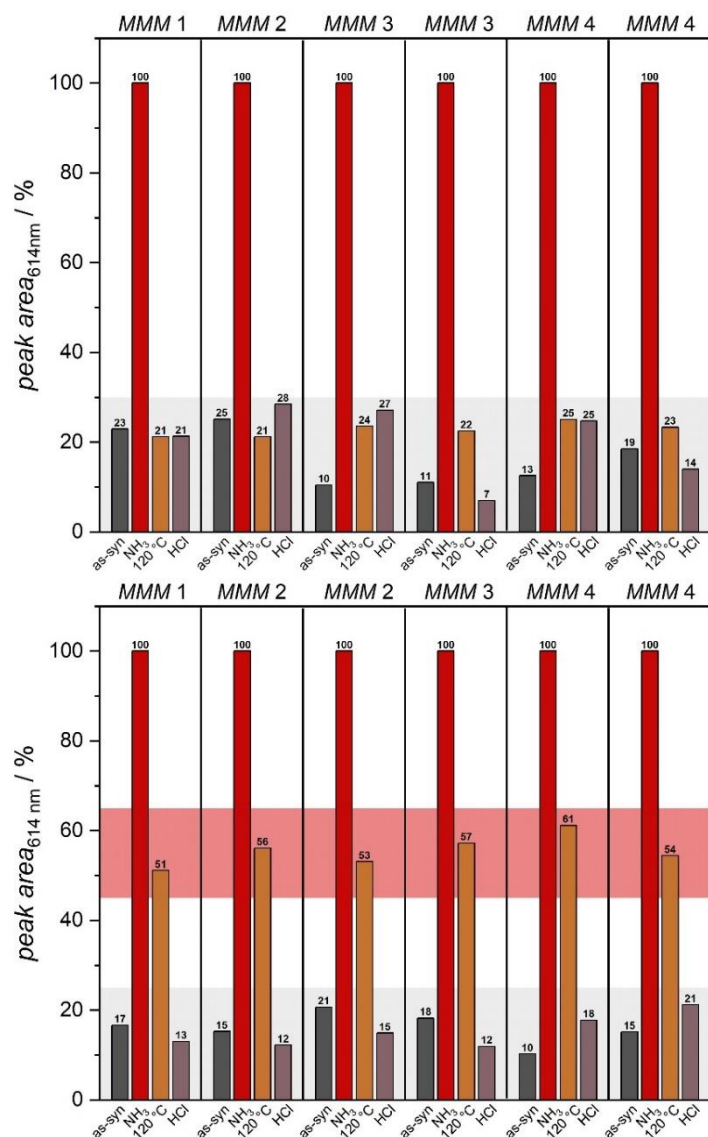


Figure S21: Calculated peak areas of the peak at 614 nm ($\lambda_{\text{ex}} = 300$ nm) after every step of read-out sequence normalized to the maximum fluorescence intensity observed after the ammonia exposure step for different batches of MMM and modified MMM of Eu,Co- (top) and Eu,Fe-MOF-808@PVDF (bottom). The areas marked in grey represent the percentage range in which the fluorescence response was defined as “turned off”. The percentage values in the area marked in red represent the read-out response which was defined as “turned on”. The fluorescence measurements were performed under N₂ flow.

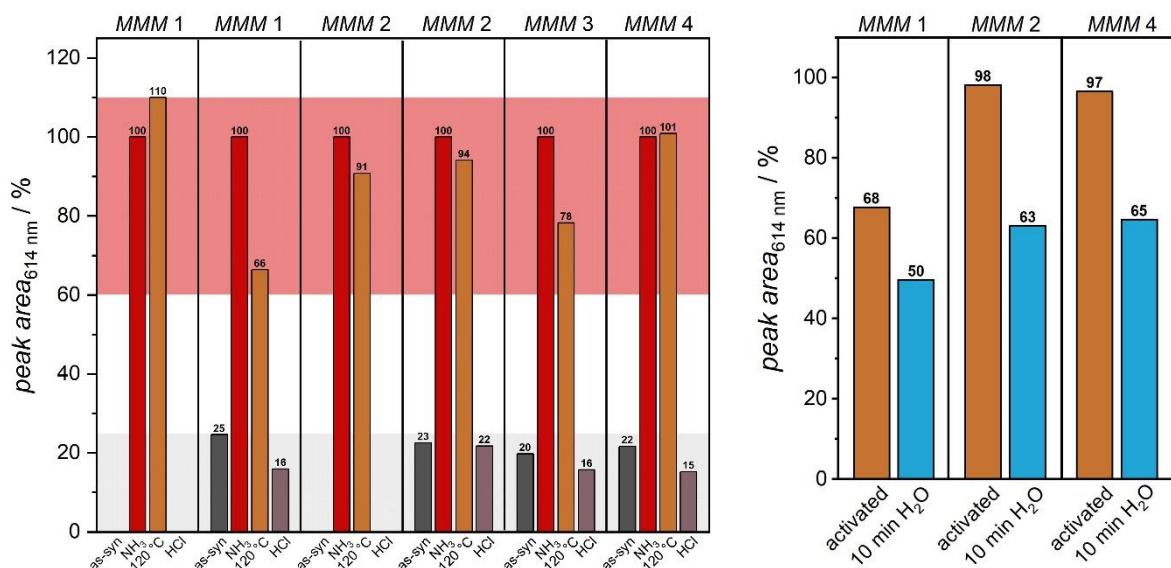


Figure S22: Calculated peak areas of the peak at 614 nm ($\lambda_{ex} = 300$ nm) after every step of the read-out sequence for different batches of MMM and modified MMM of Eu,Fe-MOF-808@PVDF without additional H₂O exposure directly after the heating step. The areas marked in grey represent the percentage range in which the fluorescence response was defined as “turned off”. The percentage values in the area marked in red represent the read-out response which show visible fluorescence (left). Comparison of the calculated peak areas after the second read-out step without (orange) and with additional water exposure after the activation step (right). The fluorescence measurements were performed under N₂ flow.

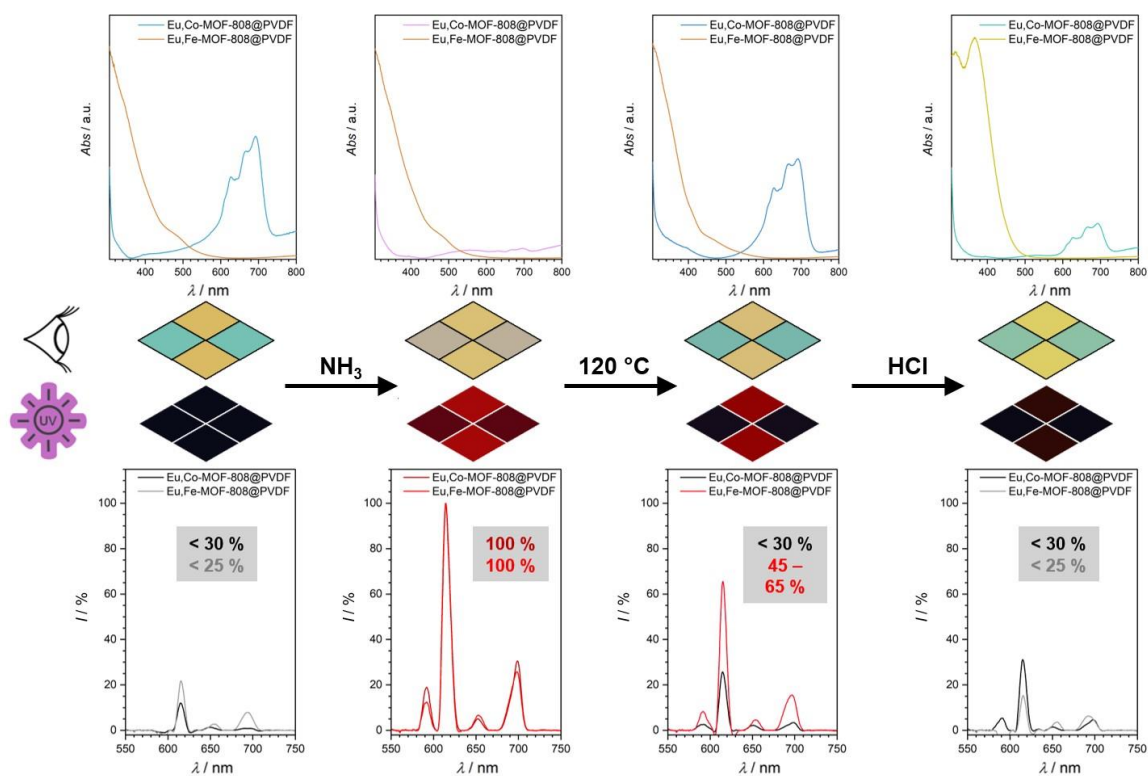


Figure S23: Color change read-out by UV-vis spectroscopy and fluorescence switching captured by a portable fluorescence spectrometer ($\lambda_{ex} = 300$ nm) in combination with the calculated read-out areas for a potential barcode made of Eu,TM-MOF-808 @PVDF pieces.

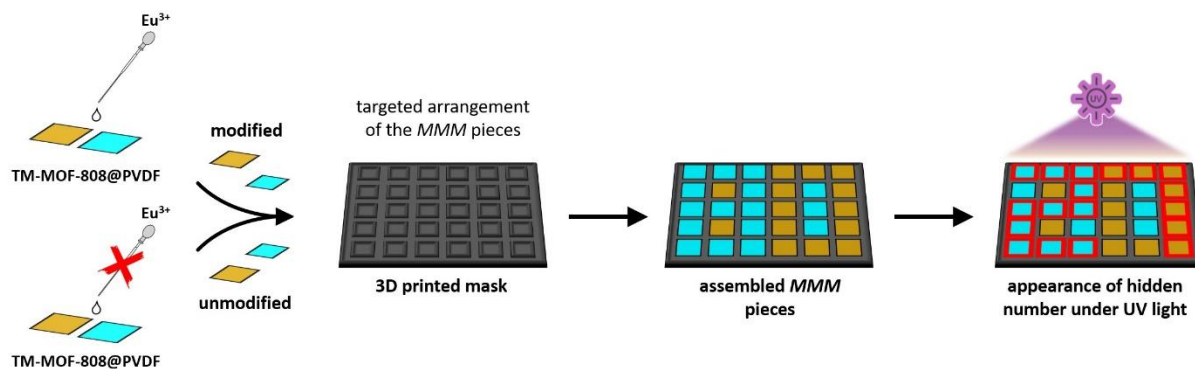


Figure S24: Schematic overview of the design of a barcode prototype made of MMM parts. Targeted arrangement of europium modified and unmodified TM-MOF-808@PVDF pieces in a 3D printed mask to assemble the number “80”. Modified and unmodified MMM cannot be distinguished by color so that numbers can be hidden within the number “80” by assembling a number from the modified ones. The number “27” appears only under UV light during the read-out process.

6 EDXS measurements of the materials

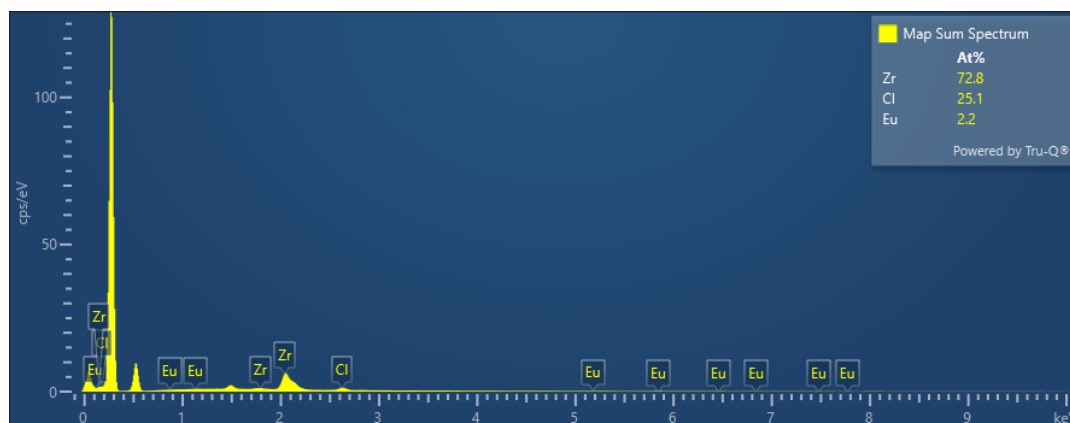


Figure S25: Exemplary EDX spectrum of Eu-MOF-808.

Table S1: Values of atomic percentage (at%) and calculated amounts of incorporated metal cations per IBU for all materials.

material	at%				Co:Zr ₆	Fe:Zr ₆	Eu:Zr ₆
	Zr	Co	Fe	Eu			
Eu-MOF-808	72.76			2.15			0.2
Co-MOF-808	52.30	5.95			0.7		
Fe-MOF-808	47.75		12.92			1.6	
Eu,Co-MOF-808	67.16	2.57		6.77	0.2		0.6
Eu,Fe-MOF-808	75.73		4.84	7.32	0.4		0.6

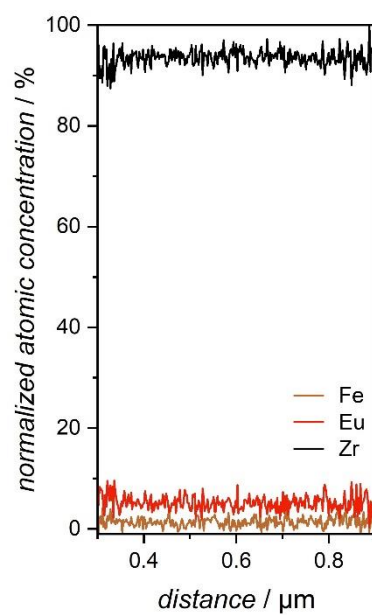
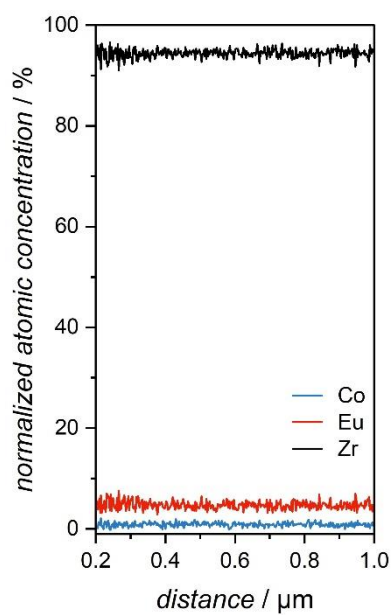
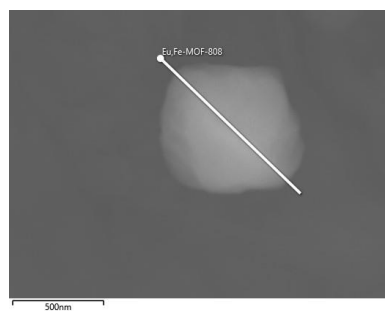
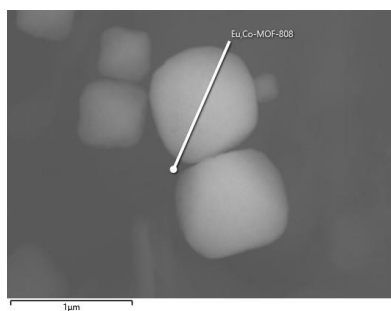


Figure S26: SEM-EDXS line scans of Eu,Co-MOF-808 (left) and Eu,Fe-MOF-808 (right) showing that the elements are uniformly distributed in the particles.